DOI: 10.1002/ejic.200900429

Molecular Iodine Stabilization in an Extended N···I–I···N Assembly

Francesco Isaia,*[a] M. Carla Aragoni,[a] Massimiliano Arca,[a] Francesco Demartin,[b] Francesco A. Devillanova,[a] Guido Ennas,[c] Alessandra Garau,[a] Vito Lippolis,[a] Annalisa Mancini,[a] and Gaetano Verani[a]

Keywords: N,S Ligands / Donor-acceptor systems / Iodine / Density functional calculations / X-ray diffraction

The adduct [bis(quinoxaline)-2,2′,3,3′-disulfide·I_2]$_\infty$ (Q_2S_2·I_2)$_\infty$ (**1**) can be easily synthesised from the reaction of Q_2S_2 and I_2 in CH_2Cl_2 or, in the absence of any solvent, through diffusion of I_2 vapours at 60 °C. X-ray diffraction analysis shows the presence of an extended N···I–I···N assembly in which each I_2 molecule links a Q_2S_2 molecule at both ends through a nitrogen atom to form a polymeric species; the *d*(I–I) and *d*(N–I) bond lengths confirm a very weak nitrogen–iodine interaction at the base of the N···I–I···N assembly. DFT calculations provide optimised distances for the N···I and I–I bonds and explanation for the zigzag chain formation: the mPW1PW functional and the B3LYP hybrid functional with a variety of basis sets for the I atomic species [CRENBL, LANL2DZ, LANL2DZ(d,p), LANL08(d), SBKJC, SBKJC polarised-LFK and Stuttgart RLC] have been tested. Compound **1** proved stable up to nearly 100 °C, and the stability is to be mainly attributed to the lattice energy of its polymeric structure then to donor–acceptor stabilisation. The facile insertion of molecular iodine into the Q_2S_2 network makes this compound an interesting iodine sponge, suitable for I_2 storage; moreover, Q_2S_2 can easily collect and release I_2(g) by a temperature-controlled process (60 and 97 °C, respectively).

Introduction

The reaction of unsaturated nitrogen heterocycles with iodine has attracted a great deal of interest in past years both in themselves and for their implications in different fields of research, which span from synthetic to biological, material and industrial chemistry.[1] These reactions can follow a variety of different pathways depending both on the nature of the heterocyclic donor and the experimental conditions used: among the possible products are the neutral (n→σ*) charge-transfer (CT) adducts between nitrogen and iodine featuring an almost linear N···I–I moiety,[1] and the extended adducts of the type N···I–I···I–I, in which the N···I–I moiety acts through the terminal iodine as a donor towards a second iodine molecule. Conversely, when the N···I–I moiety behaves as an acceptor towards another N-donor molecule, an almost linear N···I–I···N system with the I–I bridging the donor molecules have occasionally been isolated.[1]

Pennington,[2,3] and Uchida[4] studied the N···I_2 interaction of some aromatic N-donor heterocycles (Scheme 1) including pyrazine (pyz),[2] quinoxaline (quinox)[3] and phenazine (phenaz),[3,4] showing that different types of compounds can be formed depending on a number of different factors such as sterics, electronics and packing energies. In seeking to extend our studies in this area,[1d] we have focused our attention on bis(quinoxaline)-2,2′,3,3′-disulfide (Q_2S_2)[5] (Scheme 1); this compound, isolated by Dalziel and Slawinski[6] in 1968, has never been studied since for its complexing ability towards metal ions or as a Lewis donor. Q_2S_2 is an almost planar rectangular molecule (13.83 × 4.66 Å) with a highly delocalised π-electron system over the five rings and featuring four equivalent sp^2 nitrogen atoms and two sulfur atoms in the dithiine ring. We report here on the reactivity of Q_2S_2 towards the Lewis acceptors I_2, IBr and ICl, the crystal structure of the adduct Q_2S_2·I_2 and its thermal analysis. DFT calculations have

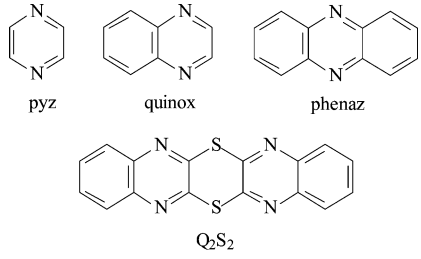

Scheme 1.

[a] Dipartimento di Chimica Inorganica ed Analitica, Università degli Studi di Cagliari, Cittadella Universitaria, 09042 Monserrato (CA), Italy
[b] Dipartimento di Chimica Strutturale e Stereochimica Inorganica, Università di Milano, Via G. Venezian 21, 20133 Milano, Italy
[c] Dipartimento di Scienze Chimiche, Università degli Studi di Cagliari, Cittadella Universitaria, 09042 Monserrato (CA), Italy
Supporting information for this article is available on the WWW under http://dx.doi.org/10.1002/ejic.200900429.

been employed to explain the nature of the donor–acceptor interaction in the N···I–I···N assembly; the mPW1PW functional and the B3LYP hybrid functional with a variety of basis sets for the I atomic species [CRENBL, LANL2DZ, LANL2DZ(d,p), LANL08(d), SBKJC, SBKJC polarised-LFK and Stuttgart RLC] have been tested to find reliable optimised distances for the I–I and N···I bonds.

Results and Discussion

Reactivity of Q_2S_2 towards I_2, IBr and ICl

Treatment of Q_2S_2 with an equivalent of I_2 in CH_2Cl_2 yielded a dark orange solution, from which an orange microcrystalline solid (**1**) of stoichiometry consistent with a Q_2S_2/I_2 ratio of 1:1 in good yield separated upon standing at ca. 10 °C. This compound features an intense ν(I–I) Raman peak at 193.5 cm^{-1} that is up-shifted by 13.5 cm^{-1} compared to solid I_2.[7,8] We investigated the formation of compound **1** by recording during 6 h a series of FT-Raman spectra in the ν(I–I) region (300–50 cm^{-1}) on a solution having a Q_2S_2 to I_2 molar ratio of 1:1 ($[Q_2S_2] = 8.80 \times 10^{-2}$ M, CH_2Cl_2). Initially, only the signal of free I_2 in solution at 208 cm^{-1} was detectable, but in the course of the reaction this signal decreased in intensity until it reached the noise level; noteworthy is that no signal related to I_2 interacting with Q_2S_2 was observed. At the same time, formation of a pale orange solid was observed, whose FT-Raman spectrum and elemental analysis confirmed to be compound **1**.

The reaction of Q_2S_2 with an equivalent of IBr in CH_2Cl_2 led to the immediate formation of a dark yellow solid, which on the basis of elemental analysis determination and FT-Raman spectroscopy (i.e., the presence of a peak at 193.5 cm^{-1}) was identified as compound **1**. Although unexpected, halogen scrambling is not unprecedented. In fact, some examples of structurally characterised 1:1 I_2 adducts of tertiary phosphanes[9a] and selonic donors[9b] have been reported to form by reaction with IBr.

Treatment of Q_2S_2 with ICl (1 equiv.) in CH_2Cl_2 resulted in the separation from the solution of a gummy dark yellow oil, which failed to crystallise on long standing. The same reaction carried out at lower temperature (≈5.0 °C) resulted in unsatisfactory results as well.

X-ray Crystal Structure Determination of $(Q_2S_2{\cdot}I_2)_\infty$

Because of the different bonding modes to the I_2 molecule inherently possible for Q_2S_2, an X-ray diffraction analysis was undertaken to firmly establish the structural features of this compound. The asymmetric unit of compound **1** (Figure 1) contains Q_2S_2 and I_2 molecules located at about two different crystallographic inversion centres. Each Q_2S_2 molecule is linked through N···I donor–acceptor interactions to two I_2 molecules to form polymeric chains made by alternating Q_2S_2 and I_2 molecules in a zigzag fashion (Figure 2). The N···I–I interactions are almost linear [177.6(1)°] with an N(2)···I distance of 2.994(2) Å shorter than the sum of the van der Waals radii for nitrogen (1.55 Å) and iodine (1.98 Å); conversely, no S···I interaction is found.

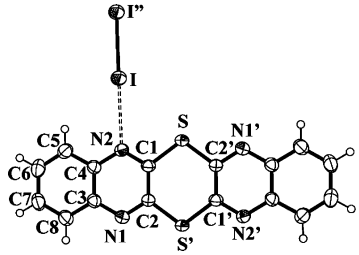

Figure 1. Structure of $Q_2S_2{\cdot}I_2$ (**1**) with numbering scheme adopted; selected bond lengths and angles are reported in Table 1. Symmetry codes: ' $-x, -y, 1-z$; " $1-x, -y, 2-z$.

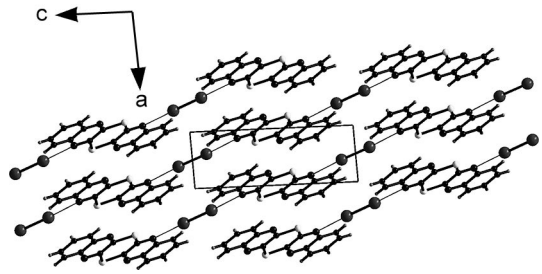

Figure 2. View of the packing diagram of **1** along [010].

Adduct formation shows little effect on the donor moiety bond lengths, while it results in an elongation of the I–I bond compared to that observed in gaseous I_2 (2.66 Å),[10a] but shorter than that found in solid I_2 (2.715 Å).[10b] The iodine molecules in **1** lie significantly out of the heterocycle plane (I atom displacement 0.59 Å), as consequence of the N(1)–N(2)–I angle of 168.5° (Table 1). The bridging I_2 displays a bond length [2.7063(7) Å] slightly shorter than those observed in complexes $(pyz{\cdot}I_2)_\infty$ [d(I–I) = 2.733(1) Å],[2] $(quinox{\cdot}I_2)_\infty$ [d(I–I) = 2.724(1) Å][3] and $(phenaz{\cdot}I_2)_\infty$ [d(I–I) = 2.726(1) Å].[3,4]

An explanation of the N–I and I–I bond lengths in the N···I–I···N systems can be based on a simplified molecular orbital (MO) description between the central I_2 molecule and the two N-donors.[8,11] The result of extending the simple n→σ* description for the donor–acceptor interaction in terminal I_2 adducts (i.e., MO combination of a lone pair from the donor with the empty σ* orbital of I_2) to a system in which an I_2 molecule bridges two donor molecules (n→σ*←n) is that only two out of the four electrons from the nitrogen atoms have a bonding nature, as the other two occupy a nonbonding orbital. In this situation, the bonding electrons are distributed over three bonds instead of two, as in terminal I_2 adducts. Consequently, the N···I bonds in the idealised N···I_2···N systems should be longer than in the simple adduct N···I_2, whereas the I–I bond should be shorter. This view is well supported by comparison of the

Table 1. Selected bond lengths, angles and thermal decomposition temperature (onset temperature) for compound **1** and related adducts featuring the N···I–I···N assembly. Gaseous and solid iodine *d*(I–I) have also been inserted.

Compound	*d*(N···I) [Å]	*d*(I–I) [Å]	N–I–I [°]	N–N–I[a] [°]	Onset temp. [°C]	Ref.
$Q_2S_2{\cdot}I_2$ (**1**)	2.994(2)	2.7063(7)	177.6(1)	168.5(1)	97	[b]
pyz·I_2	2.817(1)	2.733(1)	175.2(1)	169.4(1)	101	[2,3]
Me_4pyz·I_2	3.085(1)	2.718(1)	177.4(1)	175.4(1)	82	[2,3]
quinox·I_2	2.92(2)	2.724(1)	175.8(3)	175.6(3)	99	[3]
	2.95(2)		178.8(3)	175.5(3)		
phenaz·I_2	2.982(5)	2.726(1)	180.0(1)	180.0(1)	131	[3,4]
(9-Cl-acrid)$_2$·I_2	2.980(3)	2.742(2)	177.0(8)	165.8(1)[c]	[d]	[11]
			179.3(6)			
I_2(g)		2.66				[10a]
I_2(s)		2.715				[10b]

[a] Angle between the N···N vector (e.g., N1 and N2 in Q_2S_2) and the I···I vector. [b] This work. [c] The C···N vector is considered. [d] Data not available.

N–I and I–I bond lengths in N···I_2···N adducts (Table 1) and the terminal I_2 adduct [2,3,5,6-tetrakis(2′-pyridyl)-pyrazine·2I_2]: *d*(N–I) 2.56(8) Å, *d*(I–I) 2.750(1) Å.[1c]

DFT Calculations

In order to better understand the nature of the interaction between the donor Q_2S_2 and I_2, QM-DFT calculations have been performed on the isolated Q_2S_2 molecule and the 1:1 $Q_2S_2{\cdot}I_2$ adduct. Following recent studies reported on a variety of inorganic compounds,[12] Barone's and Adamo's mPW1PW functional[13] was paralleled to the well-known three-parameter B3LYP hybrid functional. For the heavy I atomic species, a variety of basis sets (BSs) accompanied by relativistic effective core potentials (ECPs) have been tested [CRENBL,[14] LANL2DZ,[15] LANL2DZ(d,p),[12,16] LANL08(d),[15,17] SBKJC,[18] SBKJC polarised-LFK[18,19] and Stuttgart RLC[20]]. An examination of the optimised I–I and N···I bond lengths (Table S1, Supporting Information) shows that, as previously remarked, the mPW1PW functional results in shorter bond lengths, and the trends on the distances as a function of the adopted BSs are anyway the same. Among the various combinations of functionals and BSs, the best agreement with structural data has been obtained with the recently reported completely uncontracted LANL08(d) and with the double-ζ LANL2DZ(d,p) basis sets for iodine. In particular, the calculated geometry at B3LYP/LANL08(d) provides reliable optimised distances for the I–I and N···I bonds (2.764 and 2.887 Å, respectively), with a ratio between the two values (1.05) very close to the experimental one (1.11). The optimised structure calculated for Q_2S_2 in agreement with structural data shows that the donor is entirely planar, and that the negative charge evaluated at the NBO level[21] is concentrated on the four equivalent nitrogen atoms (–0.456 e), whereas the sulfur atoms feature a positive charge (+0.370 e), thus accounting for preferring the N···I_2 interaction to the S···I_2 one. Calculations on Q_2S_2 show that HOMO and HOMO-1 (Figure 3) are π in nature molecular orbitals with large contributions from the in-phase and out-of-phase combinations, respectively, of sulfur p atomic orbitals. Interestingly, calculations performed on $Q_2S_2{\cdot}I_2$ with the iodine unit bonded by the sulfur atom show that in this adduct, which is slightly less stable than the N-bonded one (7.31 kJ mol^{-1}), the Q_2S_2 unit is not planar but folded along the S–S vector. As shown by Kohn–Sham frontier orbitals, the interaction occurs between the HOMO-2, localised mainly on the N-donor sites, and the empty pσ* orbital of I_2 (Figure 3). A comparison of the N···I and I–I bond lengths (Table S1, Supporting Information) and the evaluation of the relative lengthening of the I–I distance as compared to that calculated in the gas phase for the isolated iodine molecule[22,23] allow for an evaluation of the strength of the donor–acceptor interaction, which varies depending on the BS adopted for I. The interaction with I_2, evaluated in 49.99 kJ mol^{-1} by a second-order perturbation theory analysis of the Fock matrix, leads to a planar structure con-

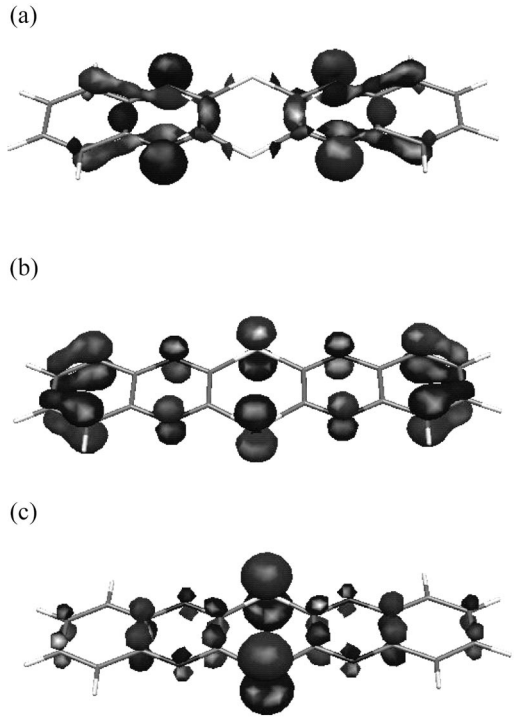

Figure 3. Frontier filled Kohn–Sham orbitals calculated for Q_2S_2 at DFT level: HOMO-2 (a), HOMO-1 (b), and HOMO (c).

taining the N···I–I linear moiety and featuring a CT from Q_2S_2 to I_2 [–0.098 e; d(N···I) = 2.887 Å], resulting in a slight decrease in the I–I bond order (Wiberg bond index[24] = 0.902). Consequently, the NBO charge distribution within the donor is modified, so that the most negatively charged nitrogen atom available for the second donation becomes N(2′) (–0.451 e), whereas the other two available donor sites N(1) and N(1′) are slightly less negative (–0.446 e). This is in agreement with the experimental structural data and seems to be a plausible explanation for the zigzag chain formation commented above.

Hanks et al.[11] have reported on the electronic properties of a system bearing the N···I–I···N assembly [(9-chloroacridine)$_2$·I_2] (see Table 1) and concluded that the stabilisation of the adduct is due more to the size and shape of the donor than to electronic factors. In fact, the crystal packing requirements that force the I–I molecule 0.73 Å out of the plane of the donor molecule causes a large decrease in the donor I_2 orbital interaction energy. Similarly in $(Q_2S_2·I_2)_\infty$ where the I–I molecule displacement is 0.59 Å, a weak nitrogen–iodine interaction is obviously expected.

Thermal Analysis of $(Q_2S_2·I_2)_\infty$ and Reactivity of Q_2S_2 with Gaseous I_2 and IBr

Investigation of the thermal behaviour of **1** (Figure 4) shows that no loss of iodine is observed at room temperature. A very small mass loss of about 1% is observed in the range 25–97 °C and is mainly related to the action of purging argon. Between 97 and 225 °C, iodine is completely eliminated with multiple mass losses: evaluation of the thermogravimetric analysis (TGA) curve yields a mass loss of 42 wt.-%, which is in agreement with the elemental analysis of compound **1**. Chemical degradation of the donor starts afterwards at a temperature above 273 °C. These measurements further confirm that the stability of I_2 in the Q_2S_2 network is mainly to be attributed to the lattice energy of its polymeric structure rather than to the N···I interactions.[11]

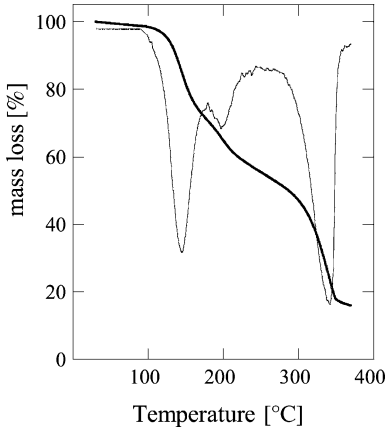

Figure 4. Thermogravimetric analysis (thick line) and corresponding derivative curves (thin line) for $Q_2S_2·I_2$ (**1**).

Because the good stability performance of the $Q_2S_2·I_2$ adduct was in the temperature range 50–70 °C, the reaction between Q_2S_2 and I_2 was also studied with the halogen in the gas phase in order to verify the role of the solvent, if any, in driving the crystallographic assembly. The solid reagents (Q_2S_2 to I_2 molar ratio = 1:3) were placed in two vials inside a degassed Aldrich pressure tube and then heated at 60 °C for 12 h. The system was cooled to room temperature and the dark red powder obtained from the reaction was investigated by FT-Raman spectroscopy. The spectrum shows a sharp peak at 193.5 cm^{-1} and a broad, more intense one at 172.0 cm^{-1},[25] the $I_{193.5}/I_{172.0}$ ratio is 0.55 (Figure 5, curve A). The former peak is exactly at the same frequency found in compound **1** and is to be related to I_2 bridging two molecules of Q_2S_2, whereas the peak at 172.0 cm^{-1} should be related to the formation of a terminal $Q_2S_2·I_2$ adduct (**2**) (through N and/or S donor atoms). In fact, in weak or medium-weak terminal bound I_2 adducts (n→σ*) [d(I–I) < 2.86 Å] the measured ν(I–I) Raman frequency shifts towards lower values (in the range 180–135 cm^{-1}) as compared to the stretching frequency of I_2 in the solid state (180 cm^{-1}) (Figure 6).[8,25]

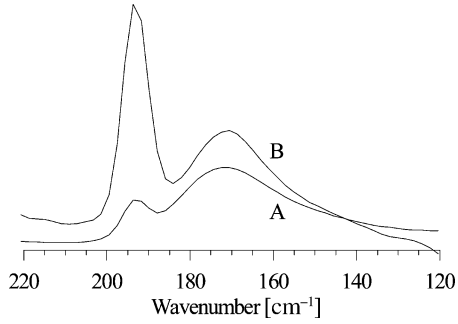

Figure 5. FT-Raman spectra in the ν(I–I) region of compound **1** obtained from the reaction of Q_2S_2 and I_2 (1:3 molar ratio) in a pressure tube: (A) after 12 h at 60 °C and (B) after 48 h at 20 °C in air.

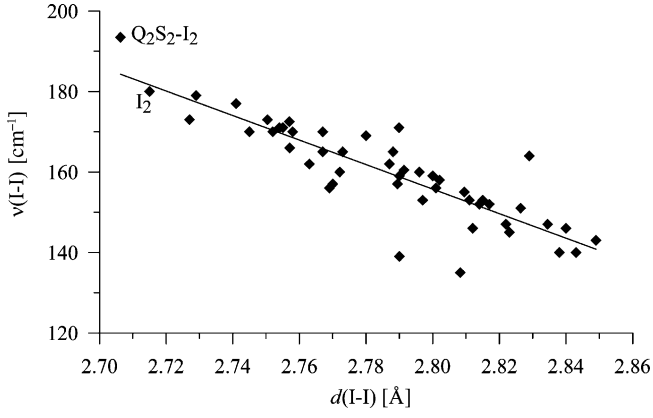

Figure 6. Scatter plot between the ν(I–I) Raman frequencies and the bond lengths d(I–I) for weak or medium weak I_2 adducts (n→σ*) {regression line: $x = d$(I–I), $y = \nu$(I–I); y = 1009.13–304.78x, R = 0.75; data from ref.[8]}. The points related to $Q_2S_2·I_2$ [(n→σ*←n) interaction] and solid I_2 have been introduced in the regression.

Interestingly, a sample kept at 20 °C in air for 48 h shows that the intensity of the peak at 172.0 cm^{-1} decreased significantly (Figure 5, curve B; $I_{193.5}/I_{172.0}$ = 2.8), stating the decomposition of **2**, which is not surprising because of the weak nature of the adduct. Moreover, after washing the sample with *n*-hexane and sonication (1 min) to crush it further, the Raman peak at 172.0 cm^{-1} almost disappears. Elemental analysis of this powder was found satisfactory for $Q_2S_2{\cdot}I_2$ stoichiometry. The reaction of Q_2S_2 with IBr in the gas phase carried out as previously reported for I_2 did not result in satisfactorily results, as sticky, oily products were formed. No attempts were made to use ICl under these reaction conditions.

Conclusions

The novel adduct $(Q_2S_2{\cdot}I_2)_\infty$ (**1**) can be easily synthesised from the reaction of Q_2S_2 and I_2 or IBr in CH_2Cl_2. It can also be prepared in the absence of any solvent, through diffusion of I_2 vapours at 60 °C. Each I_2 molecule links a Q_2S_2 molecule at both ends through a nitrogen atom to form a polymeric species; the bond lengths and angles in the donor are substantially unaffected compared to those of the free Q_2S_2; the *d*(I–I) and *d*(N–I) bond lengths confirm a very weak nitrogen–iodine interaction at the base of the N···I–I···N assembly. In spite of this, compound **1** proved stable up to nearly 100 °C, the stability of I_2 in the Q_2S_2 network is mainly to be attributed to the lattice energy of its polymeric structure rather than to the N···I interactions. DFT calculations at the B3LYP level using LANL08(d) basis sets provide reliable optimised distances for the N···I and I–I bonds and correctly explain the assembly of Q_2S_2 and I_2 molecules in a zigzag fashion. The facile insertion of molecular iodine into the Q_2S_2 network makes this compound an interesting iodine sponge, suitable for I_2 storage considering also that samples of **1** still proved stable at room temperature after two years. Q_2S_2 can easily collect and release I_2(g) by a temperature-controlled process (60 and 97 °C, respectively), opening new perspectives to **1**, and more in general to N···I–I···N based compounds.

Experimental Section

Materials and Instrumentation: Reagents were used as purchased from Aldrich. FT-Raman spectra were recorded with a Bruker FRS 100/S Fourier transform Raman spectrometer, operating with a diode-pumped Nd:YAG exciting laser emitting at 1064 nm. Thermogravimetric analysis was performed with a TGA7 Perkin–Elmer instrument. A few milligrams of sample were inserted into the TGA instrument and held isothermically at room temperature (25 °C) for 1 h. The samples were then heated from room temperature to 400 °C at 10 °C min^{-1} with an argon flow rate of 60 mL min^{-1}.

Synthesis of $(Q_2S_2{\cdot}I_2)_\infty$ (1): Bis(quinoxaline)-2,2′,3,3′-disulfide[6] (0.115 g, 0.39 mmol) in CH_2Cl_2 (70 mL) and I_2 (0.100 g, 0.39 mmol) in CH_2Cl_2 (30 mL) were reacted at room temperature for 4 h, then the filtered solution was allowed to stand at 10 °C for 2 d; the product was obtained as dark orange crystals. Yield: 150 mg, 70%. $C_{16}H_8I_2N_4S_2$ (574.18): calcd. C 33.47, H 1.40, N 9.76, S 11.17; found C 33.5, H 1.5, N 9.8, S 11.3. Raman: $\tilde{\nu}$ = 193.5 [ν(I–I)] cm^{-1}.

Crystallography: Intensity data were collected at room temperature (Nonius CAD4 diffractometer) with graphite monochromated Mo-K_α (λ = 0.71073 Å) radiation up to 2θ = 50°. The structure was solved by direct methods with SIR97[26a] and the refinement was carried out on F^2 SHELXL97[26b] with anisotropic displacement parameters for non-hydrogen atoms and including all the hydrogen atoms. Crystal data: $C_{16}H_8I_2N_4S_2$, M = 574.18, triclinic, space group $P\bar{1}$, a = 4.103(1) Å, b = 8.751(2) Å, c = 11.983(3) Å, α = 99.66(2)°, β = 92.17(2)°, γ = 93.12(2)°, U = 423.1(2) $Å^3$, Z = 1, $D_{calcd.}$ = 2.254 g cm^{-3}, μ(Mo-K_α) = 3.969 mm^{-1}, wR_2 = 0.0405, R = 0.0161 [1315 absorption-corrected reflections with $I > 2\sigma(I)$].

CCDC-713418 (for **1**) contains the supplementary crystallographic data for this paper. These data can be obtained free of charge from The Cambridge Crystallographic Data Centre via www.ccdc.cam.ac.uk/data_request/cif.

Computation: Quantum-chemical calculations were performed on Q_2S_2, on I_2 and on the $Q_2S_2{\cdot}I_2$ adduct, both N- and S-bonded, with the commercial suite of programs Gaussian03[27] at DFT level with the B3LYP and mPW1PW[13] functionals. For C, H, N, and S atomic species the double-ζ plus polarisation (pVDZ) all-electron basis sets by Schäfer et al.[28] was used, whereas for I several basis sets with relativistic effective core potential sets were adopted [CRENBL, LANL2DZ, LANL2DZ(d,p), LANL08(d), SBKJC, SBKJC polarised-LFK and Stuttgart RLC].[14–20] All basis sets were obtained the EMSL basis set library.[29] NBO populations[21] and Wiberg bond indices[24] were calculated at the optimised geometries. The programs Gabedit 2.0.7[30] and Molden 4.7[31] were used to investigate charge distributions and molecular orbital shapes. All calculations were performed on an E4 workstation equipped with four AMD Opteron quad-core processors and 16 Gb of RAM.

Supporting Information (see footnote on the first page of this article): Optimised I–I and N···I bond lengths for the 1:1 adduct $Q_2S_2{\cdot}I_2$.

Acknowledgments

Dr. Maria Bonaria Carrea is acknowledged for her contribution to this work.

[1] a) E. L. Rimmer, R. D. Bailey, W. T. Pennington, T. W. Hanks, *J. Chem. Soc. Perkin Trans. 2* **1998**, 2557–2562; b) R. Bailey Walsh, C. W. Padgett, P. Metrangolo, G. Resnati, T. W. Hanks, W. T. Pennington, *Cryst. Growth Des.* **2001**, *1*, 165–175 and references cited therein; c) R. D. Bailey, M. Grabarczyk, T. W. Hanks, W. T. Pennington, *J. Chem. Soc. Perkin Trans. 2* **1997**, 2781–2786; d) M. C. Aragoni, M. Arca, F. A. Devillanova, M. B. Hursthouse, S. L. Huth, F. Isaia, V. Lippolis, A. Mancini, G. Verani, *Eur. J. Inorg. Chem.* **2008**, 3921–3928 and references therein.

[2] R. B. Bailey, M. L. Buchanan, W. T. Pennington, *Acta Crystallogr., Sect. C* **1992**, *48*, 2259–2262.

[3] R. B. Bailey, G. W. Drake, M. Grabarczyk, T. W. Hanks, L. L. Hook, W. T. Pennington, *J. Chem. Soc. Perkin Trans. 2* **1997**, 2773–2779.

[4] T. Uchida, K. Kimura, *Acta Crystallogr., Sect. C* **1984**, *40*, 139–140.

[5] Chemical name: [1,4]dithiino[2,3-*b*;5,6-*b*′]diquinoxaline; synonym: 6,13-dithia-5,7,12,14-tetraazapentacene.

[6] J. A. W. Dalziel, A. K. Slawinski, *Talanta* **1968**, *15*, 1385–1389.

[7] Raman spectroscopy has been widely used to understand the nature of the products isolated in the solid state between donors and I_2: a) M. Arca, M. C. Aragoni, F. A. Devillanova, A. Garau, F. Isaia, V. Lippolis, A. Mancini, G. Verani, "Reactions Between Chalcogen Donors and Dihalogens/Interalogens: Typology of Products and Their Characterization by FT-Raman Spectroscopy", *Bioinorg. Chem. Appl.* **2006**, Article 58937. DOI:10.1155/BCA/2006/58937 and references cited therein.
[8] V. Lippolis, F. Isaia in *Handbook of Chalcogen Chemistry: New Perspectives in Sulfur, Selenium and Tellurium* (Ed.: F. A. Devillanova), RSC Publishing, **2007**, ch. 8.2, pp. 477–499.
[9] a) P. D. Boyle, W. I. Cross, S. M. Godfrey, C. A. McAuliffe, R. Pritchard, S. Teat, *J. Chem. Soc., Dalton Trans.* **1999**, 2219–2224; b) F. Cristiani, F. A. Devillanova, F. Isaia, V. Lippolis, G. Verani, *Inorg. Chem.* **1994**, *33*, 6315–6324.
[10] a) A. F. Wells in *Structural Inorganic Chemistry*, Oxford University Press, **1987**, ch. 9, p. 385; b) F. van Bolhuis, P. B. Koster, T. Migchelsen, *Acta Crystallogr.* **1967**, *23*, 90–93.
[11] E. L. Rimmer, R. D. Bailey, T. H. Hanks, W. T. Pennington, *Chem. Eur. J.* **2000**, *6*, 4071–4081.
[12] a) S. Virko, T. Petrenko, A. Yaremko, R. Wysokinsky, D. Michalska, *J. Mol. Struct.* **2002**, *602*, 137–142; b) A. Soran, H. J. Breunig, V. Lippolis, M. Arca, C. Silvestru, *Dalton Trans.* **2009**, 77–85; c) C. Gabbiani, A. Casini, L. Messori, A. Guerri, M. A. Cinellu, G. Minghetti, M. Corsini, C. Rosani, P. Zanello, M. Arca, *Inorg. Chem.* **2008**, *47*, 2368–2379.
[13] C. Adamo, V. Barone, *J. Chem. Phys.* **1998**, *108*, 627–631.
[14] L. A. La John, P. A. Christiansen, R. B. Ross, T. Atashroo, W. C. Ermler, *J. Chem. Phys.* **1987**, *87*, 2812–2824.
[15] P. J. Hay, W. R. Wadt, *J. Chem. Phys.* **1985**, *82*, 270–310.
[16] A. Luna, S. Gevrey, J. Tortajada, *J. Chem. Phys.* **2000**, *104*, 110–118.
[17] a) L. E. Roy, P. J. Hay, R. L. Martin, *J. Chem. Theory Comput.* **2008**, *4*, 1029–1031; b) C. E. Check, T. O. Faust, J. M. Bailey, B. J. Wright, T. M. Gilbert, L. S. Sunderlin, *J. Phys. Chem. A* **2001**, *105*, 8111–8116.
[18] a) W. J. Stevens, M. Krauss, H. Basch, P. G. Jasien, *Can. J. Chem.* **1992**, *70*, 612–630; b) R. Cundari, W. J. Stevens, *J. Chem. Phys.* **1993**, *98*, 5555–5565.
[19] N. P. Labello, A. M. Ferreira, H. A. Kurtz, *Int. J. Quantum Chem.* **2006**, *106*, 3140–3148.
[20] W. Kuechle, M. Dolg, H. Stoll, H. Preuss, *Mol. Phys.* **1991**, *74*, 1245–1263.
[21] a) A. E. Reed, F. Weinhold, *J. Chem. Phys.* **1983**, *78*, 4066–4073; b) A. E. Reed, R. B. Weinstock, F. Weinhold, *J. Chem. Phys.* **1985**, *83*, 735–746; c) A. E. Reed, L. A. Curtiss, F. Weinhold, *Chem. Rev.* **1988**, *88*, 899–926.
[22] Optimized I–I bond lengths for the isolated iodine molecule in the gas phase (B3LYP functional): 2.824, 2.863, 2.716, 2.718, 2.823, 2.786 and 2.853 Å calculated with the CRENBL, LANL2DZ, LANL2DZ(d,p), LANL08(d), SBKJC, SBKJC polarized-LFK and Stuttgart RLC BSs, respectively.
[23] Optimized I–I bond lengths for the isolated iodine molecule in the gas phase (mPW1PW functional): 2.777, 2.830, 2.683, 2.685, 2.789, 2.756 and 2.819 Å calculated with the CRENBL, LANL2DZ, LANL2DZ(d,p), LANL08(d), SBKJC, SBKJC polarized-LFK and Stuttgart RLC BSs, respectively.
[24] K. Wiberg, *Tetrahedron* **1968**, *24*, 1083–1096.
[25] P. Deplano, F. A. Devillanova, J. R. Ferraro, F. Isaia, V. Lippolis, M. L. Mercuri, *Appl. Spectrosc.* **1992**, *11*, 1625–1629.
[26] a) A. Altomare, M. C. Burla, M. Camalli, G. L. Cascarano, C. Giacovazzo, A. Guagliardi, A. G. G. Moliterni, G. Polidori, R. Spagna, *J. Appl. Crystallogr.* **1999**, *32*, 115–119; b) G. M. Sheldrick, *SHELX97-Program for Crystal Structure Analysis (Release 97–2)*, University of Göttingen, Germany, **1998**.
[27] M. J. Frisch, G. W. Trucks, H. B. Schlegel, G. E. Scuseria, M. A. Robb, J. R. Cheeseman, J. A. Montgomery Jr., T. Vreven, K. N. Kudin, J. C. Burant, J. M. Millam, S. S. Iyengar, J. Tomasi, V. Barone, B. Mennucci, M. Cossi, G. Scalmani, N. Rega, G. A. Petersson, H. Nakatsuji, M. Hada, M. Ehara, K. Toyota, R. Fukuda, J. Hasegawa, M. Ishida, T. Nakajima, Y. Honda, O. Kitao, H. Nakai, M. Klene, X. Li, J. E. Knox, H. P. Hratchian, J. B. Cross, V. Bakken, C. Adamo, J. Jaramillo, R. Gomperts, R. E. Stratmann, O. Yazyev, A. J. Austin, R. Cammi, C. Pomelli, J. W. Ochterski, P. Y. Ayala, K. Morokuma, G. A. Voth, P. Salvador, J. J. Dannenberg, V. G. Zakrzewski, S. Dapprich, A. D. Daniels, M. C. Strain, O. Farkas, D. K. Malick, A. D. Rabuck, K. Raghavachari, J. B. Foresman, J. V. Ortiz, Q. Cui, A. G. Baboul, S. Clifford, J. Cioslowski, B. B. Stefanov, G. Liu, A. Liashenko, P. Piskorz, I. Komaromi, R. L. Martin, D. J. Fox, T. Keith, M. A. Al-Laham, C. Y. Peng, A. Nanayakkara, M. Challacombe, P. M. W. Gill, B. Johnson, W. Chen, M. W. Wong, C. Gonzalez, J. A. Pople, *Gaussian 03*, Gaussian, Inc., Wallingford, CT, **2004**.
[28] A. Schafer, H. Horn, R. Ahlrichs, *J. Chem. Phys.* **1992**, *97*, 2571–2576.
[29] a) D. J. Feller, *Comput. Chem.* **1996**, *17*, 1571–1586; b) K. L. Schuchardt, B. T. Didier, T. Elsethagen, L. Sun, V. Gurumoorthi, J. Chase, J. Li, T. L. Windus, *J. Chem. Inf. Model.* **2007**, *47*, 1045–1052.
[30] A. R. Allouche, *Gabedit* is a free Graphical User Interface for computational chemistry packages. It is available from http://gabedit.sourceforge.net/.
[31] G. Schaftenaar, J. H. Noordik, *J. Comput.-Aided Mol. Des.* **2000**, *14*, 123–134.

Received: May 11, 2009
Published Online: July 8, 2009

